Characterization and modeling of thin-layer drying of cocoyam slices

Owoidoho Michael, Nkem[1*], Ayobami Olayemi, Oladejo[2], Akindele Folarin, Alonge[3]

(Department of Agricultural and Food Engineering, Faculty of Engineering, University of Uyo, P.M.B 1017, Uyo, Akwa Ibom State, Nigeria)

Abstract: Convective hot air drying of cocoyam slices was investigated at different drying temperature (40 to 90 °C) and slice thickness (2, 4 and 6 mm) at an air velocity of 1 $m\,s^{-1}$. The effect of drying temperature and slice thickness on the drying characteristics and drying time were determined to study the effects of heat on processed cocoyam. Mathematical modeling of the thin layer drying process was performed using eight thin layer drying models. The models were tested for validity using coefficient of determination (R^2), chi square (χ^2) and root mean square error (RMSE). The effect of the drying temperature on the color of dried cocoyam was also investigated. The color was measured using CIE L* a* b* method. The results showed that, increasing the drying air temperature and decreasing slice thickness reduces the drying time of cocoyam. The effective moisture diffusivity increased with increase in drying temperature and the biot number (Bi_m) of cocoyam at temperature of 40 to 70 °C were less than 0.1 while that of 80 to 90 °C were in the range of $0.1 < Bi_m < 100$. The activation energy obtained at 40 to 90 °C was 37.92 kJ. The Page model was found to be best fit for the drying kinetics of cocoyam. The largest color difference was observed at 90 °C compared to the fresh sample. Increase in temperature reduced the brightness and yellowness of cocoyam.

Keywords: drying kinetics, mass transfer, color, cocoyam slices.

Citation: Nkem, O. M., A. O. Oladejo, and A. F. Alonge. 2023. Characterization and modeling of thin-layer drying of cocoyam slices. Agricultural Engineering International: CIGR Journal, 25(3): 237-257.

1 Introduction

Cocoyam (*Xanthosoma sagittifolium*) is a viable food commodity with appreciable nutritional profile, higher productivity, and better storability compared to other indigenous roots and tubers as well as having potential as a sustainable food security measure in the West African sub-region. Cocoyam contributes significant portion of the carbohydrate content of the diet in many regions in developing countries and provide edible starchy storage corms or cormels (Kabuo et al., 2018). Cocoyam has more crude protein than other root and tuber crops and contains reasonable amount of calcium, phosphorus, vitamin A and B, its starch is also highly digestible because of the small size of the starch granules (Kabuo et al., 2018). Cocoyam, like other tuber crops are prone to deterioration if not properly stored. To ensure safe storage over longer

Received date: 2022-11-26 **Accepted date:** 2023-03-03

***Corresponding author: Owoidoho Michael Nkem**, Department of Agricultural and Food Engineering, Faculty of Engineering, University of Uyo, P.M.B 1017, Uyo, Akwa Ibom State, Nigeria, 08137715914, Owoidohonkem@gmail.com.

period without the risk of losses from rotting, the cocoyam corms are dried to obtain shelf stable products.

Drying depicts a complex process of heat and mass transfer of removing moisture from biological products. In food processing, the main role of drying technologies is to preserve agricultural commodities quality, extend their shelf life and produce new products that would not otherwise be feasible (Desa et al., 2019). Drying as a method of food preservation, decreases the moisture content and water activity of the crop to minimize chemical, biochemical and microbiological deterioration thereby improving food stability. Several methods of drying have been used in drying of agricultural produce such as sun drying, oven drying, solar drying, vacuum drying, convective hot air drying among others (Figiel and Michalska, 2017). Convective hot air drying is a complex process of simultaneous transfer of mass (moisture removal from the surface of the food material being dried) and heat (from the hot air to the surface of the food) from fruits, vegetables and medicinal plants (Agrawal and Methekar, 2017). The simulation of drying experimental results with help of empirical and semi-empirical models is valuable for designing new or in improving existing drying systems. They are also helpful in drying process configuration and control (Hssaini et al., 2021). In engineering, mathematical modeling is a prerequisite to successfully simulate or scale up the whole process of drying for optimization or control of the operating conditions. It is an inevitable part of design, development and optimization of a dryer (Inyang et al., 2018).Mathematical modeling mainly involve elaborative study of drying kinetics, which describe the mechanisms and the influence that certain process variables exert on moisture transfer (Inyang et al., 2018). In other words, it can be used to study the drying variables, evaluate the drying kinetics and to optimize the drying parameters and the conditions. A proper drier design requires knowledge on the characteristics of the material to be dried and the drying kinetics. Several thin-layer drying models have been widely used to describe drying characteristics of agricultural products. These are theoretical, semi-theoretical, and empirical models. Among these, semi-theoretical and empirical models which take into account the external resistance to moisture transport process between the material and atmospheric air, provide a greater extent of accurate results, give a better prediction of drying process behaviors, and make less assumptions due to their reliance on experimental data are the most widely used (Onwude et al., 2016). Several researchers have worked on mathematical modeling and experimental studies on the thin-layer drying of various vegetables and fruits, such as root vegetables and onion (Górnicki et al., 2020), pumpkin sample (Sadeghi et al., 2019), yam slices (Kamal et al., 2020), yellow cassava (Oladejo, 2020), banana peel (Tai et al., 2021), figs fruit (Hssaini et al., 2021) among others. Appearance is one of the most important sensory quality attributes of food which can affect consumer's acceptance toward them as well as purchase intent (Renata et al., 2022). Color and appearance are often the initial criteria used by consumers to judge the quality of food and they can influence food consumption and purchases (Renata et al., 2022). There are fewer studies on kinetics color change of cocoyam (*Xanthosoma sagittifolium*) slices due to drying temperature. Hence, this study was aimed to investigate the thin-layer drying characteristics of cocoyam slices and characterize cocoyam color due to temperature differences.

2 Materials and methods

2.1 Materials

Healthy Cocoyam (*Xanthosoma sagittifolium*) corms were harvested from a local farm in Uruan located between latitude 6° 40W and longitude 7° 30E in the north western part of Akwa Ibom State, Nigeria. All the samples were harvested within 8-10 months of

planting (the maturation period of *Xanthosoma sagittifolium*), sample that were not damaged or attacked by pests were selected. Cocoyam corms were cleaned to remove soil particles and other debris and peeled manually with stainless steel knife. The peeled cocoyam corms were sliced to 2, 4 and 6 mm thickness using a food slicing machine. The average weight of each slice was ± 5 g and the geometry of the sample was slab-shaped. The initial moisture content of cocoyam as determined using the AOAC (2000) was 73.43% (wet basis).

Thin layers of cocoyam were dried using a convective air oven using temperature of 40 °C, 50 °C, 60 °C, 70 °C, 80 °C and 90 °C (Figure 1). The dimensions of the dryer were 40 cm wide, 43 cm high and 72 cm long. The oven is consisted of heating unit, centrifugal fan, drying chamber and temperature control unit. The movement of the air was cross flow (side to side) at a velocity of $1\ m\ s^{-1}$ and it flowed parallel to the surface of the samples. The moisture loss was taken every 30 min until equilibrium moisture content was attained.

2.2 Drying Experiment

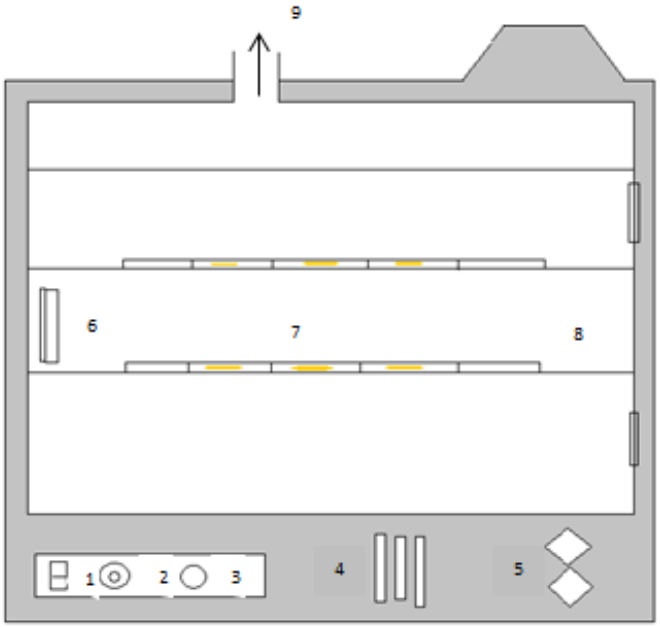

Figure 1 Schematic diagram of the dryer used in the experiment

2.2.1 Determination of moisture ratio and drying rate

The moisture ratio (M_R) and drying rate (D_R) of cocoyam slices were calculated using the following Equations 1 (Erbay and Icier, 2010).

$$M_R = \frac{M_t - M_e}{M_0 - M_e} \quad (1)$$

Where M_t, M_0, and M_e are moisture contents at any time in the drying process, the initial moisture content, and the equilibrium moisture content (kg water per kg dry matter), respectively, and t is the drying time (min). The value of M_e is relatively small for long drying times, compared to values of M_t and M_0, so the Equation 1 can be simplified to Equation 2. The drying rate was calculated from Equation 3 (Rayaguru and Routray, 2010).

$$M_R = \frac{M_t}{M_0} \quad (2)$$

$$\text{Drying rate, } D_R = \frac{M_{t+\Delta t} - M_t}{\Delta t} \quad (3)$$

Where $M_{t+\Delta t}$ is moisture content at $t + \Delta t$ (kg water per kg dry matter), t is time (min) and Δt is the change in time of drying.

2.2.2 Determination of effective moisture diffusivity

Considering that convective hot air drying process of cocoyam takes place in the falling rate period (Ndukwu et al., 2017; Afolabi et al., 2015), the variation of moisture content with time can be

mathematically described by Fick's second law of diffusion given in Equation 4.

$$\frac{\partial M}{\partial t} = D_{eff}\frac{\partial^2 M}{\partial x^2} \quad (4)$$

Where M is the local moisture content (kg water per kg dry matter), t is the time (s), x is material dimension (m) and D_{eff} is the effective moisture diffusivity ($m^2 s^{-1}$). If it is assumed that the moisture migrates only by diffusion, that the system is isotropic, that the solid matrix has no shrinkage during processing and that the final moisture content is equal to its equilibrium moisture (M_e) at the drying conditions, Equation 4 can be solved for a thin layer slab geometry (Onwude et al., 2016) to obtain the Equation 5:

$$MR = \frac{M_t - M_e}{M_0 - M_e} = \frac{8}{\pi^2}\sum_{n=0}^{\infty}\frac{1}{(2n+1)^2}\exp\left(-\frac{(2n+1)^2\,\pi^2 (D_{eff})t}{4h^2}\right) \quad (5)$$

Where M_R the moisture ratio and h is the half-thickness of the slab (m) and n is the positive integer. For a long drying time, Equation 5 can be simplified to the first term of the series and can be further converted into a straight-line equation as shown in Equation 6 (Oladejo et al., 2021):

$$\ln(MR) = \ln\left(\frac{8}{\pi^2}\right) - \frac{\pi^2 D_{eff} t}{4h^2} \quad (6)$$

The moisture diffusivity was calculated from the slope of the graph by plotting experimental drying data in terms of $\ln(MR)$ versus drying time.

$$slope = \frac{\pi^2 D_{eff}}{4h^2} \quad (7)$$

2.2.3 Estimation of activation energy

Effective moisture diffusivity can be related with temperature by Arrhenius expression as shown in Equation 8 (Saxena and Dash, 2015):

$$D_{eff} = D_o \exp\left(-\frac{E_a}{R\,(T+273.15)}\right) \quad (8)$$

Where D_o is a constant in the Arrhenius equation ($m^2\ s^{-1}$), E_a is the activation energy ($kJ \cdot mol^{-1}$), T is temperature of air (℃), and R is the universal gas constant (R=8.31451 $J \cdot mol^{-1} \cdot K^{-1}$). However, Equation 8 can be rearranged to form Equation 9.

$$In\left(D_{eff}\right) = In(D_o) - \frac{E_a}{R\,(T+273.15)} \quad (9)$$

$In\left(D_{eff}\right)$ as a function of *1/ (T+273.15)* was plotted to produce a straight line with a slope equal to ($\frac{E_a}{R}$), hence, E_a was estimated.

2.2.4 Determination of biot number and mass transfer coefficient

To know the type of resistance (internal and external) to mass transfer that took place during the drying of cocoyam, biot number mass transfer was taken into consideration. According to Demirel and Turhan (2003), it is expressed as Equation 10.

$$\mathrm{Bi_m} = \frac{h_m h}{D_{eff}} \quad (10)$$

Where Bi_m is the biot number mass transfer (dimensionless), h_m is the mass transfer coefficient ($m\,s^{-1}$), h is the characteristic dimension (half thickness length of the slab-shaped sample, m). Also, according to Dincer and Hussain (2002), biot number is given as:

$$\mathrm{Bi_m} = \frac{24.848}{\mathrm{Di}^{0.375}} \quad (11)$$

And,

$$D_i = \frac{y}{kh} \quad (12)$$

Where D_i is the dimensionless Dincer number, y is the flow velocity (ms^{-1}) of the drying air, and k is the drying constant (s^{-1}), which is the slope in Equation 7.

2.2.5 Modeling of experimental data

Data derived from drying of cocoyam slices were fitted to eight thin-layer drying models as shown in Table 1. Semi-theoretical models derived from Newton's law of cooling (Newton and Page models) and Fick's second law of diffusion (Henderson and Pabis, Logarithmic and Two-term exponential models) were selected while the empirical model selected were Wang and Singh model, Silva *et al* model and Peleg model. The moisture contents were expressed on dry basis, which is more convenient for modeling.

The fitness quality of the model was determined by using the coefficient of correlation (R^2), chi square (χ^2)

and root mean square error (RMSE). These parameters were calculated using the equations given in Table 2. The best model was chosen as one who has the highest coefficient of determination (R^2) and lowest root mean square error (RMSE) and chi squared (χ^2) value (Onwude et al., 2016).

Table 1 Selected Thin layer models applied to drying kinetics of cocoyam corms

S/N	Model Name	Equation	References
1	Henderson and Pabis	$MR = \mathrm{a}.\exp(-kt)$	Meisami-Asl et al. (2010); Hashim et al. (2014)
2	Logarithmic	$MR = \mathrm{a}.\exp(-kt) + c$	Rayaguru and Routray (2012); Kaur and Singh (2014)
3	Page	$MR = \exp(-kt^n)$	Akoy (2014); Tzempelikos et al. (2014)
4	Two-term exponential	$MR = a.\exp(-kt) + (1-a)\exp(-kat)$	Dash et al. (2013)
5	Wang and Singh	$MR = 1 + at + bt^2$	Omolola et al. (2014)
6	Peleg	$MR = 1 - \frac{t}{a+bt}$	Da Silva et al. (2015)
7	Silva and others model	$MR = \exp(-at - b\sqrt{t})$	Da Silva et al. (2014)
8	Newton	$MR = \exp(-kt)$	El-Beltagy et al. (2007)

Table 2 Statistical measures used for evaluating goodness of fit selected models

S/N	Statistical Measures	Formula
1	Root mean squared error	$RMSE = \sqrt{\frac{\sum_{i=1}^{N}(MR_{pre,i} - MR_{exp,i})^2}{N}}$
2	Chi squared or reduced Chi squared	$\chi^2 = \sum_{i=1}^{N}\frac{(MR_{pre,i} - MR_{exp,i})^2}{N-n}$
3	Coefficient of determination	$R^2 = \frac{\sum_{i=1}^{N}(MR_{exp,i} - MR_{pre,i})^2}{\sum_{i=1}^{N}(MR_{pre,i} - MR_{exp,i})^2}$

Note: Where $MR_{exp,i}$ is the ith experimentally observed moisture ratio $MR_{pre,i}$ is the ith predicted moisture ratio, N is the number of observations, $MR_{exp,ave}$ is the average experimentally observed moisture ratio and n is the number of experimental data points.

2.3 Color measurement

The color of fresh and dried cocoyam slices was measured using a colorimeter (CHN Spec CS 10, China) for determination of color parameters. Before each measurement, the colorimeter was calibrated against standard tile (that is, white and black). The high and low values of L*, a* and b* stand for whiteness–blackness, redness–greenness and yellowness–blueness, respectively. The Chroma values or saturation index were determined using Equation 13 (Wiktor et al., 2016).

$$C* = \sqrt{a^{*2} + b^{*2}} \quad (13)$$

The total color difference and browning index were computed using Equation 14 and Equation 15, respectively (Wiktor et al., 2016).

$$\Delta E = \sqrt{(L_0 - L^*)^2 + (a_0^* - a^*)^2 + (b_0^* - b^*)^2} \quad (14)$$

$$B.I = \frac{100(x-0.31)}{0.17} \quad (15)$$

Where

$$x = \frac{(a^* + 1.75L^*)}{(5.645L^* + a^* - 3.012b^*)} \quad (16)$$

Where ΔE = total color difference, B.I = browning index. The high and low values of L*, a* and b* stand for whiteness–blackness (100 = light, 0 = dark), redness–greenness (100 = red, −80 = green) and yellowness–blueness (100 = yellow, −80 = blue), respectively. The nought subscript refers to the color values of the fresh cocoyam. The higher the values of ΔE, the greater the color difference from the fresh

cocoyam. The Hue angle was also calculated using Equation 17 (Wiktor et al., 2016).

$$h^0 = tan^{-1}\frac{b}{a} \quad (17)$$

2.4 Statistical analysis

Data were subjected to one-way analysis of variance (ANOVA) using SPSS software version 22.0 (SPSS Inc. Chicago, U.S.A). Significant differences within drying temperature were determined at $p<0.05$ (95% confidence level). Tukey's multiple range tests was employed for comparison of means where significant differences occurred within the drying temperature combinations in terms of the responses. Graphs were plotted using Microsoft excel 2010.

3 Results and discussion

3.1 Effect of temperature on the drying kinetics of cocoyam corms

The drying curves of cocoyam slices at the different temperature and thickness are shown in Figure 2. The result showed that increasing the drying air temperature decreases the drying time of the product for all the material thickness used. At the material thickness of 2 mm, the total time for drying at 40 °C was 990 min while at 50 °C the drying time reduced to 840 min. This implied the reduction in drying time as the temperature of drying is increased. The reduction in drying due to temperature increase was also observed for material thickness of 4 mm and 6 mm. The lowest drying time (210 min) was obtained at temperature of 90 °C. The percentage reduction of drying time increased with increase in temperature compared to 40 °C (15 %, 18 %, 42, 67 and 79 % for 50, 60, 70, 80 and 90 °C respectively).

The reduction in drying time due to the increase in the drying temperature may be due to the increase of the vapor pressure within the product which may results in faster migration of moisture to the product surface. Correia et al. (2015) reported a reduction in the drying time of tomatoes with temperature range between 40 and 80 °C as the temperature was increased. Meisami-Asl et al. (2010) also observed a reduction in the drying time of apple slices when the temperature was increased from 40 to 80 °C. Similar observations were reported for *Colocasia esculenta* variety of cocoyam (Afolabi et al., 2015) and other crops by researchers (Onwude et al., 2016; Correia et al., 2015).

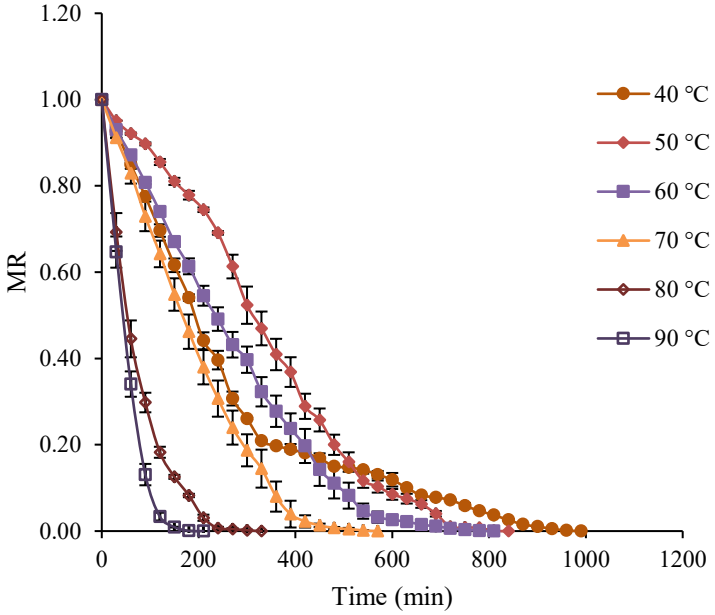

(a) 2mm

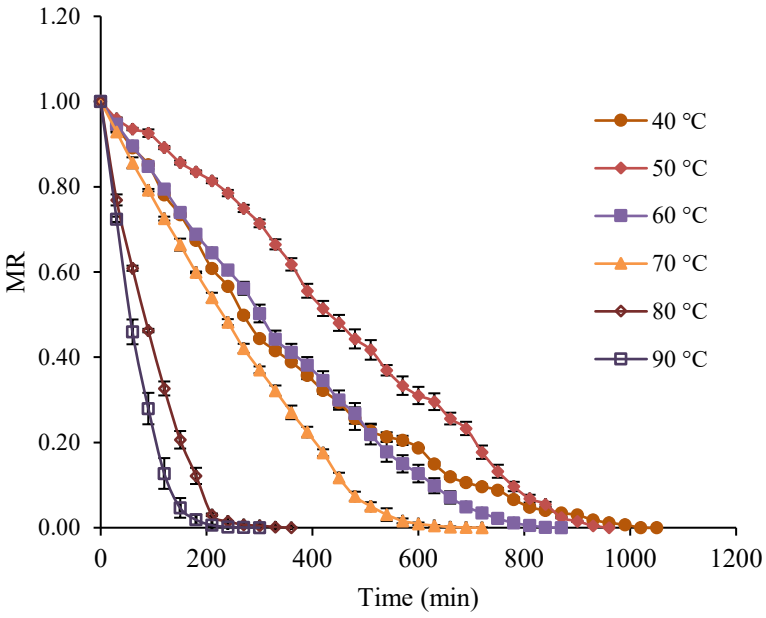

(b) 4mm

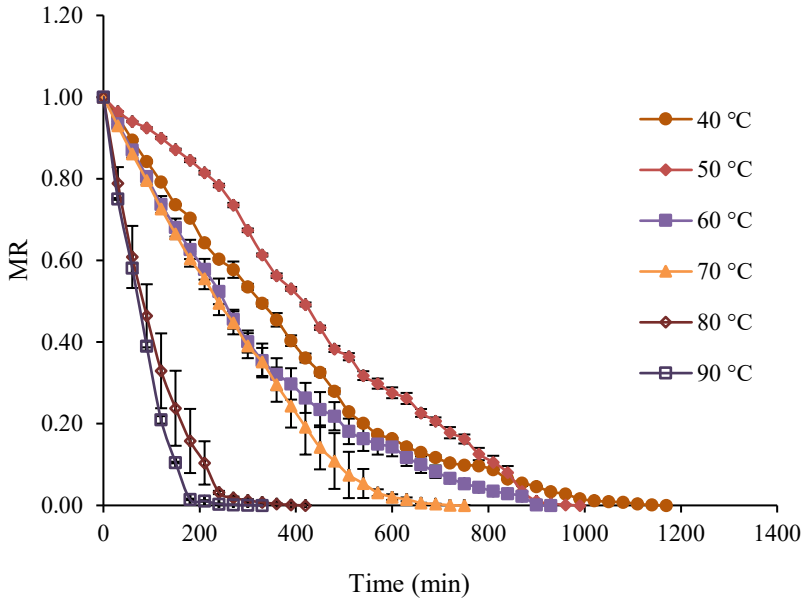

(c) 6mm

Figure 2 Moisture ratio versus time for convective drying of cocoyam slices at different temperature for (a) 2 mm (b) 4 mm and (c) 6 mm slice thicknesses.

From Figure 2 it was observed that the thin layer drying curve showed a falling rate period with decrease in moisture ratio with drying time. The falling rates explain that the dominant diffusion mechanism involved in the drying of cocoyam corms in a convective hot air dryer is liquid and vapor diffusion. The falling rate period of drying of agricultural product is controlled largely by the product being dried and is dependent upon the movement of the moisture within the material from the center to the surface by liquid diffusion which shows that the mechanism of drying is diffusion controlled (Alonge and Adeboye, 2012; Oladejo, 2020). Similar results have been observed in the drying of different fruits and vegetables: Kiwifruit

(Simal et al., 2005); sweet potato (Dinrifo, 2012), corn and wheat (Zielinska and Cenkowski, 2012) and apple pomace (Wang et al., 2007).

Alonge and Adeboye (2012) reported an initial constant rate and subsequent falling rate when drying pepper, okro and vegetable sample in a solar dryer. The determining factor in the dominant mechanism of drying is the moisture content and the structure of the food material being dried (Taylor, 2010). The determination of the dominant mechanism is important in modeling the process of drying.

The effect of temperature on the drying rate curves for 2, 4 and 6 mm material thickness is shown in Figure 3. It was observed that drying rate increased with increase in temperature and reached its maximum value at the maximum drying temperature of 90 °C used in this study. Meisami-Asl et al. (2010) also reported the highest drying rate at 80 °C when drying apple slices. It was also observed that the drying rate increased with increase in the moisture ratio. The highest drying rate reached was 0.0313, 0.0228 and 0.0207 kg per kg dry matter · min at the temperature of 90 °C, for 2, 4 and 6 mm slice thickness, respectively.

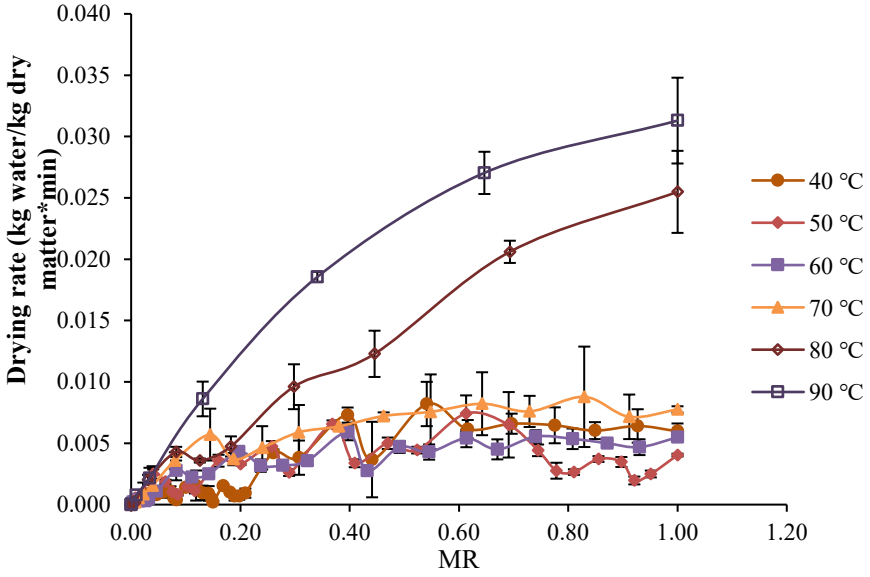

(a) 2mm

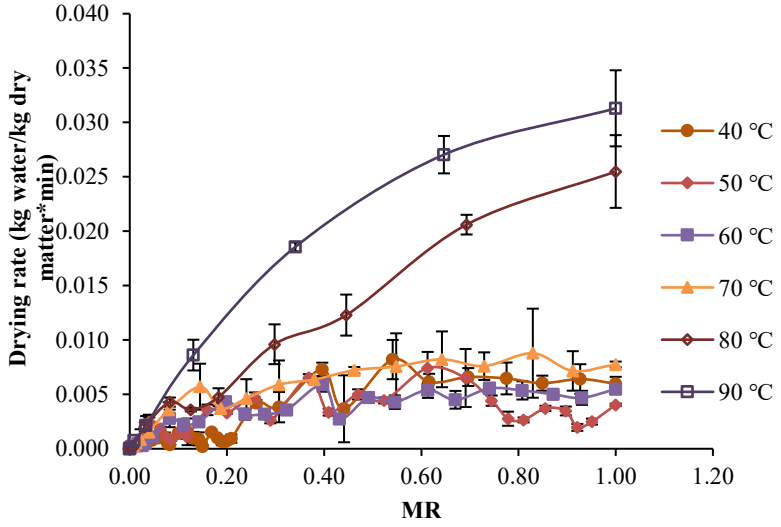

(b) 4mm

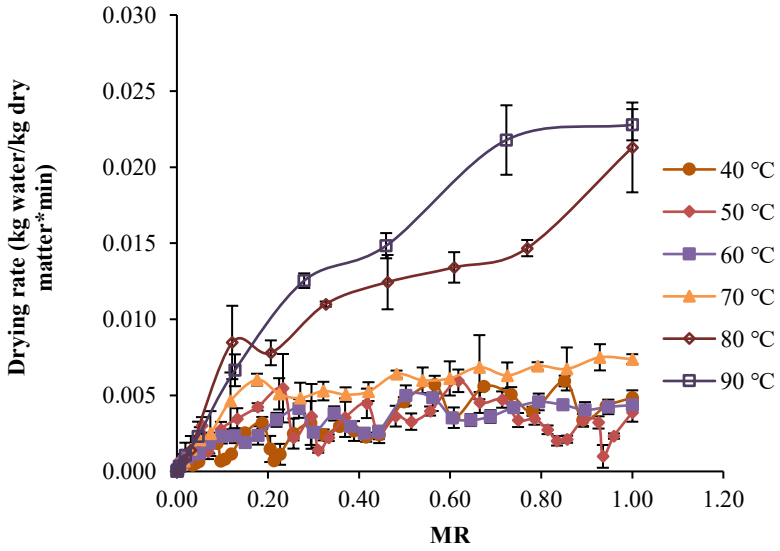

(c) 6mm

Figure 3 Drying rate curves of convective drying of cocoyam at different temperature for (a) 2 mm (b) 4 mm and (c) 6 mm slice thicknesses

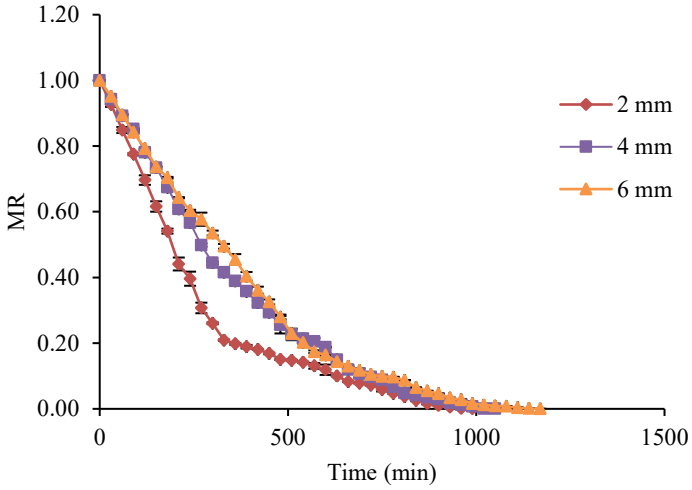

(a) 40℃

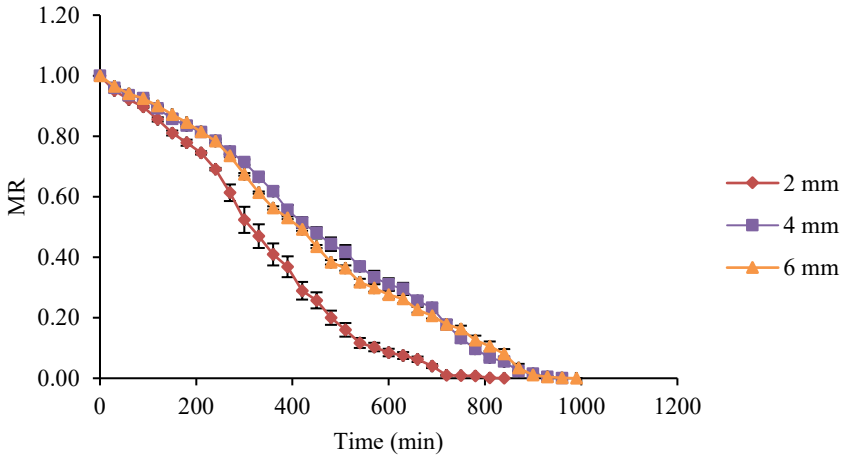

(b) 50℃

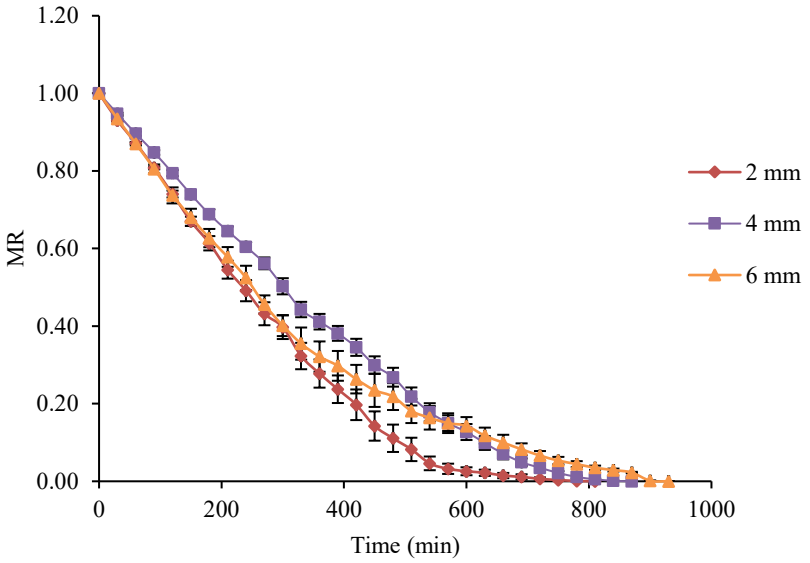
1.20
1.00
0.80
0.60
0.40
0.20
0.00
MR
0
200
400
600
800
1000
Time (min)
2 mm
4 mm
6 mm

(c) 60℃

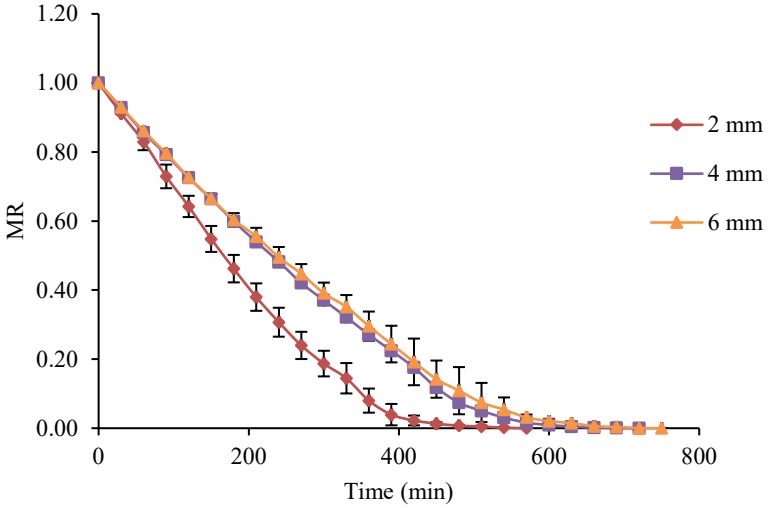
1.20
1.00
0.80
0.60
0.40
0.20
0.00
MR
0
200
400
600
800
Time (min)
2 mm
4 mm
6 mm

(d) 70℃

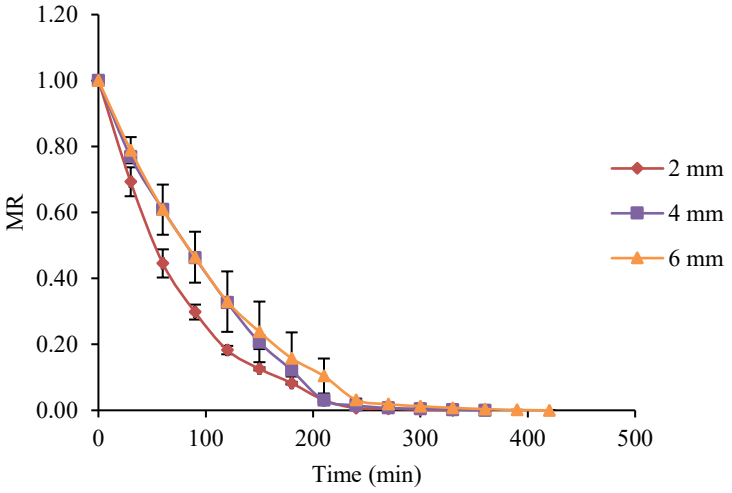
1.20
1.00
0.80
0.60
0.40
0.20
0.00
MR
0
100
200
300
400
500
Time (min)
2 mm
4 mm
6 mm

(e) 80℃

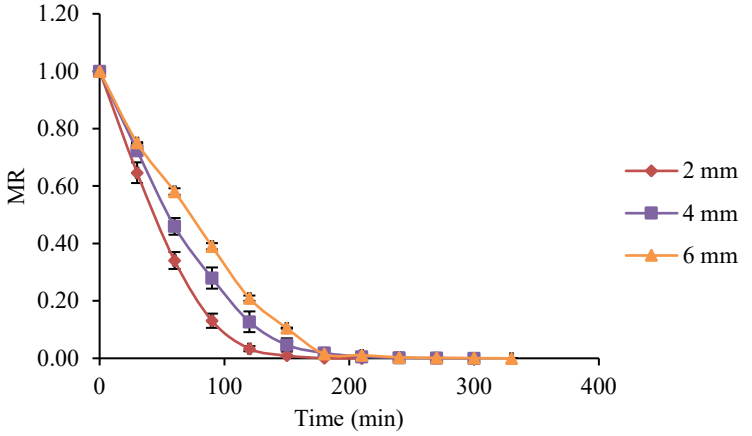

(f) 90℃

Figure 4 Moisture ratio versus time for convective drying of cocoyam slices at different thicknesses

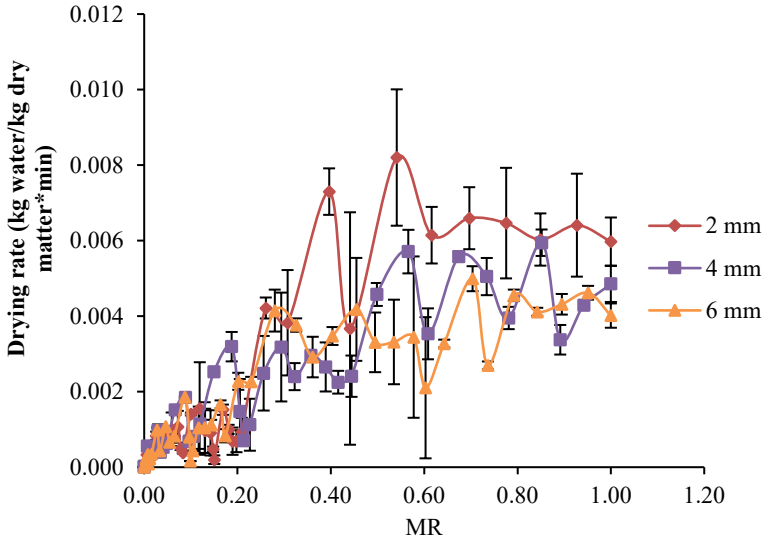

(a) 40℃

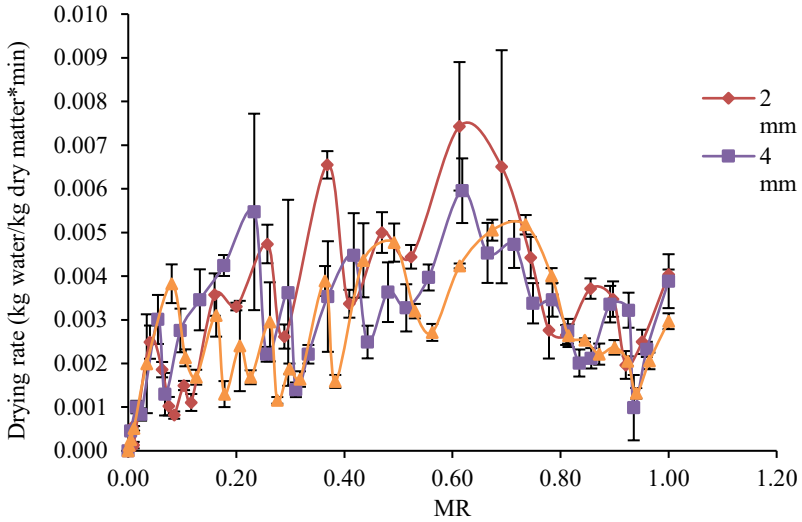

(b) 50℃

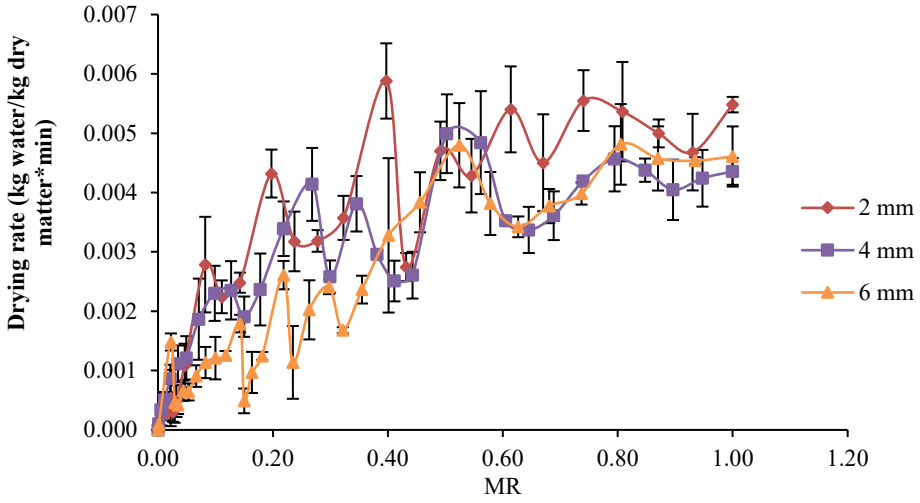
Drying rate (kg water/kg dry matter*min)
0.007
0.006
0.005
0.004
0.003
0.002
0.001
0.000
0.00
0.20
0.40
0.60
0.80
1.00
1.20
MR
2 mm
4 mm
6 mm

(c) 60℃

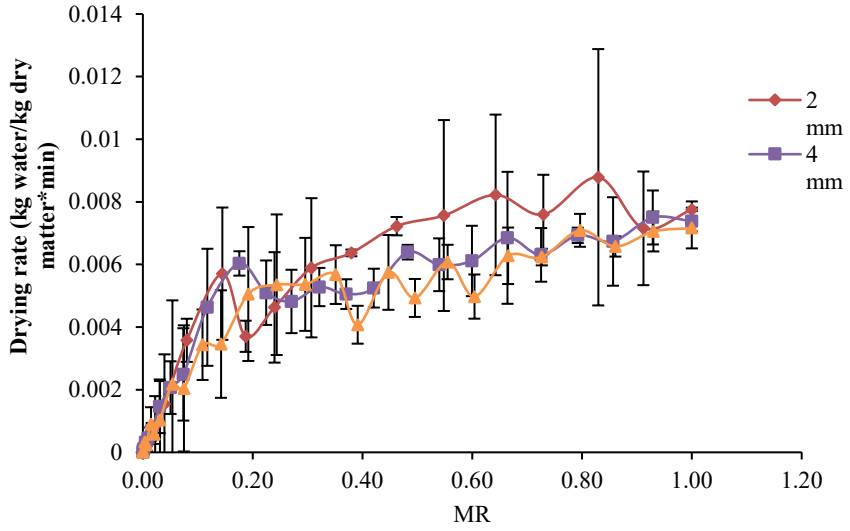
Drying rate (kg water/kg dry matter*min)
0.014
0.012
0.01
0.008
0.006
0.004
0.002
0
0.00
0.20
0.40
0.60
0.80
1.00
1.20
MR
2 mm
4 mm

(d) 70℃

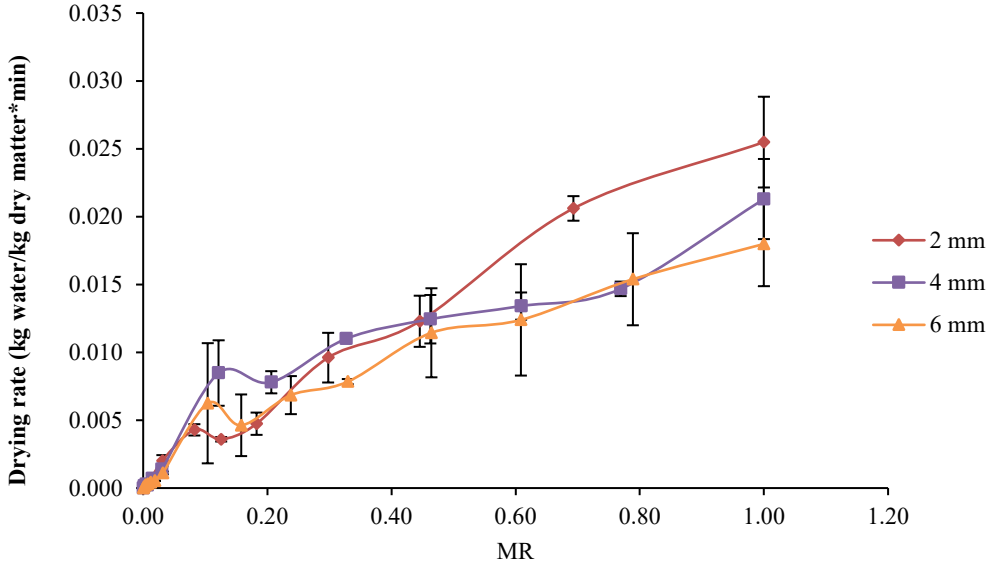
Drying rate (kg water/kg dry matter*min)
0.035
0.030
0.025
0.020
0.015
0.010
0.005
0.000
0.00
0.20
0.40
0.60
0.80
1.00
1.20
MR
2 mm
4 mm
6 mm

(e) 80℃

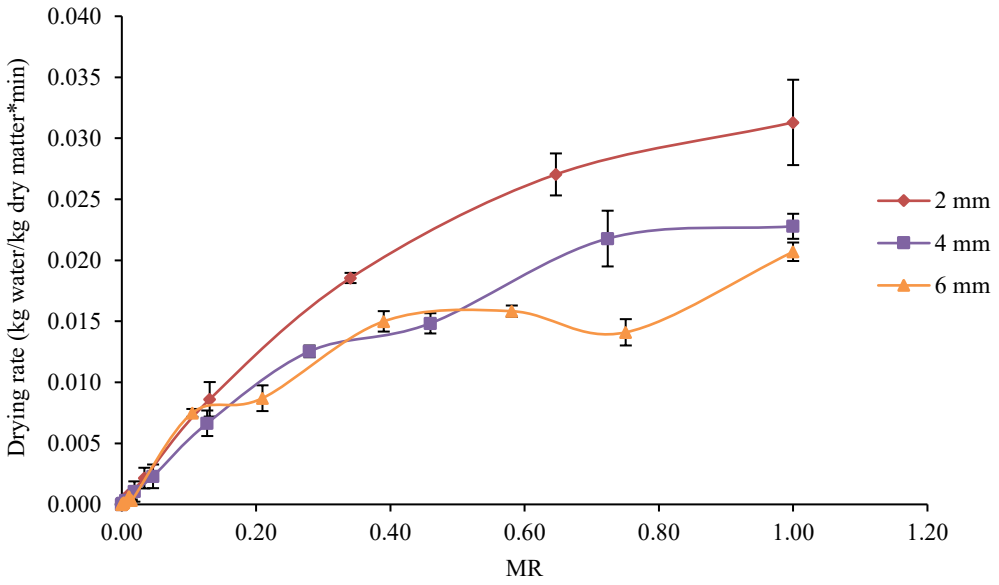

(f) 90℃

Figure 5 Drying rate curves for convective drying of cocoyam slices at different thicknesses for (a) 40 ºC (b) 50 ºC (c) 60 ºC (d) 70 ºC (e) 80 ºC and (f) 90 ºC

3.2 Effect of slice thickness on the drying kinetics of cocoyam corms

It was observed that, one of the main factors influencing the drying kinetics of the product, during the falling rate drying period, is the material thickness (Onwude et al., 2016). Increase in the material thickness increases the drying time for the convective hot air drying of cocoyam corms (Figure 4) for all cases of drying temperature. At 40 °C, the drying time increased from 990 min to 1180 min as the material thickness was increased from 2 mm to 6 mm. The result of the drying process expressed as dimensional moisture ratio built from resulting weight loss data and plotted against the drying time showed that drying experiment were proceeded in falling rate period and here was no constant rate observed. The total drying time increased by 6 and 19% when the thickness was increased from 2 mm to 6 mm. The increasing drying time due to increase in material thickness could be due to the increase in the amount of water and a longer route for moisture migration to the product surface.

The effects of slice thickness were studied for apple (Sacilik et al., 2006; Meisami-Asl et al., 2010), coconut (Madamba, 2003), flax fiber (Ghazanfari et al., 2006) and it was observed that the drying time increased with increase in thickness. Hence thickness plays a very important role in drying. It is assumed that the temperature distribution at thin layer is uniform due to the thin structure of the fruit or vegetable that has been sliced before drying.

The effect of thickness on the drying rate is shown in Figure 5 for all drying temperature. The drying rate increased with decrease in the material thickness. Material thickness of 2 mm had the highest drying rate. The highest drying rate of 0.031 kg per kg dry matter · min was obtained at the temperature of 90 °C. Hence, both the temperature and slice thickness have effect on the drying rate. Similar results have been reported for apple slices (Meisami-Asl et al., 2010). To obtain the highest drying rate, it is suggested that the temperature of drying be increased while the thickness is reduced.

3.3 Effect of drying temperature on effective moisture diffusivity, mass transfer coefficient and biot number of cocoyam slices

The results of the effective moisture diffusivity of cocoyam slices 40 to 90 °C are presented in Table 3. The value ranged from 1.171×10^{-10} to $7.603 \times 10^{-10} m^2 s^{-1}$ with $R^2 > 0.90$. Ndukwu et al. (2017)

observed similar result when investigating the heat and mass transfer parameter in the drying of cocoyam slices.

The moisture diffusivity increased with increase in drying temperature. The highest value of moisture diffusivity ($7.603 \times 10^{-10}\, m^2\, s^{-1}$) was obtained at 90 °C. There was no significant difference ($p > 0.05$) between the moisture diffusivity of samples dried at 40 and 50 °C. There was significant increase in the moisture diffusivity as the temperature increased to 90 °C. This showed that high temperature enhanced the movement of water during convective hot air drying. Hence, effective moisture diffusivity is affected by product's temperature (Erbay and Icier, 2010). The total diffusivity of the drying was due to liquid and vapour diffusion phases. At the initial stage of the drying process, when the sample contains a high quantity of moisture, the physical mechanism that governs the moisture transfer is liquid diffusion. As drying progresses, the sample is progressively dried and contains lower moisture. Hence, a porous structure is formed and the transfer of moisture is vapour (Çağlar et al., 2009).

Table 3 Effect of temperature on effective moisture diffusivity, mass transfer coefficient and biot number

Temp. (°C)	D_{eff} $(\times 10^{-10})(m^2\, s^{-1})$	R^2	h_m $(\times 10^{-8})(m\, s^{-1})$	Bi_m
40	1.171^a	0.931	0.396^a	0.0676^a
50	1.256^a	0.913	0.436^{ab}	0.0695^a
60	1.651^b	0.917	0.637^b	0.0769^b
70	2.543^c	0.916	1.150^c	0.0905^c
80	5.433^d	0.952	3.267^d	0.1203^d
90	7.603^e	0.963	5.186^e	1.1364^e

Note: Means in the same column bearing different superscript differed significantly (p<0.05).

The convective mass transfer coefficient at different drying temperature is shown in Table 3. There was no significant difference (p>0.05) between the mass transfer coefficient of samples dried at 40, and 50 °C as well as 50 and 60 °C. Other temperature showed significant increase in the mass transfer coefficient with increase in temperature. Hence, the convective mass transfer increased with increase in drying temperature. These values were similar to those obtained by Ndukwu et al. (2017) for *colocasia esculenta*. The relative humidity of the drying air at higher temperature was less compared to lower temperature, the difference in the partial pressure between the product slices and their surroundings was greater for higher temperature drying environment which resulted in a higher moisture transfer rate (Darvishi et al., 2015).

The Biot number (Bi_m) relates the ratio of internal heat conduction or mass diffusion in solids to the external convection (Darvishi et al., 2015). Hence determining biot number shows the type of resistance (internal and external) responsible for the drying mechanism. When Bi_m is less than 0.1, the external resistance dominates the transfer; when it is greater than 100, the internal resistance dominates and when Bi_m falls between 0.1 and 100, both the internal and external resistances dominate (Oladejo, 2020; Dincer and Hussain, 2002). Table 3 shows that the values of Bi_m obtained from this work for 40 to 70°C were lower than 0.1 and Bi_m for 80 and 90°C fell between 0.1 and 100. Hence, internal and external mass transfer resistance was responsible for the drying mechanism at 80°C and 90°C while external resistance dominated the drying at 40°C to 70°C. However, there was no significant difference (p>0.05) between the biot number at 40°C and 50°C. The biot number also increased significantly as the temperature increased.

When samples were dried at higher temperature, increased heating energy would increase the activity of water molecules, resulting in higher mass transfer rate. Hence, low temperature lead to low drying rate and mass flux within the material (Darvishi et al., 2015). The biot number showed that the drying of cocoyam

was divided into two phases: the first is a controlled process of evaporation of water from the surface of the dried material into the drying air ($Bi_m < 0.1$, external resistance) and the second phase ($Bi_m \geq 0.1$, internal and external resistances) is controlled by a diffusion of moisture from the centre of the material to the surface (Table 3). Similar result for Bi_m of 0.101-0.181 were reported for hot air drying of sliced melon at 40 -70 °C (Darvishi et al., 2015) and 0.0942-0.111 for hot air drying of yellow cassava slices at 70 °C (Oladejo, 2020).

3.4 Effect of drying temperature on activation energy

The activation energy for diffusion (E_a) obtained for cocoyam in this study was 37.92 kJ (Figure 6). The value of E_a shows the sensibility of the moisture diffusivity against temperature and the greater value of E_a mean more sensibility of moisture diffusivity to temperature (Erbay and Icier, 2010). Hence, the diffusivity in this study is highly dependent on temperature. Most activation energy presented in literature ranged from 14.42 to 43.26 $kJ \cdot mol^{-1}$ with large concentration found in the range of 2.6 to 39.03 $kJ \cdot mol^{-1}$ (Onwude et al., 2016). Ndukwu et al. (2017) reported similar value range of 16.16 to 42.99 kJ for varieties of cocoyam.

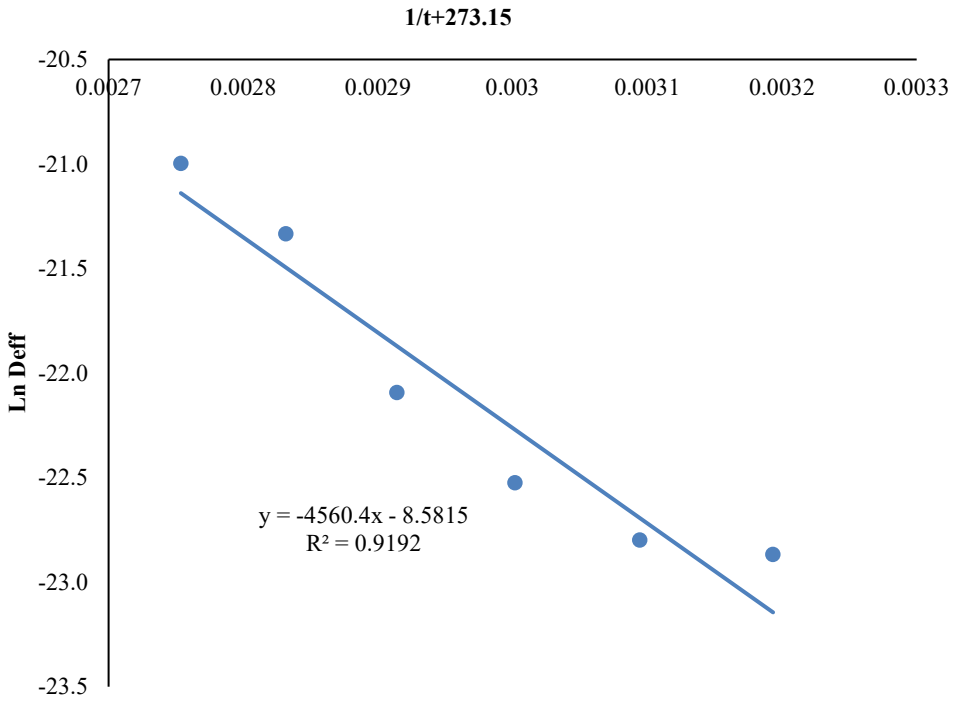

Figure 6 Arrhenius-type relationship between effective diffusivity and temperature

3.5 Mathematical modeling of the drying kinetics of convective hot-air drying

In order to determine the best model that described the drying kinetics of cocoyam slices during convective hot air drying, the experimental moisture ratio was subjected to eight drying models (Henderson and Pabis, Logarithmic, Page, Newton, Two-term Exponential, Wang and Singh, Peleg, Silva and others model). The models were validated using the coefficient of correlation (R^2), chi square (x^2) and root mean square error (RMSE). The best model was selected based on the highest R^2 value and lowest RMSE, and x^2 values. According to the results of the statistical measures for evaluating the best model for thickness of 2, 4 and 6 mm, the Page model best fitted the thin layer drying of cocoyam (Table 4) within the temperature range of 40 to 90 °C. The drying constants and coefficient for Page model is shown in Table 5.

Table 4 Average values of statistical parameters of drying for different models for cocoyam at different thickness within the temperature of 40 to 90 °C

Model Name	2 mm			4 mm			6 mm		
	χ^2	R^2	RMSE	χ^2	R^2	RMSE	χ^2	R^2	RMSE
Henderson and Pabis	0.008	0.973	0.050	0.002	0.967	0.191	0.003	0.973	0.051
Logarithmic	0.001	0.977	0.031	0.001	0.994	0.022	0.001	0.992	0.027
Page	0.001	0.996	0.019	0.001	0.994	0.019	0.001	0.996	0.020
Two-term exponential	0.004	0.964	0.050	0.005	0.959	0.064	0.004	0.963	0.136
Wang and Singh	0.002	0.981	0.040	0.001	0.994	0.024	0.001	0.993	0.026
Peleg	0.002	0.982	0.043	0.002	0.989	0.035	0.002	0.985	0.038
Silva *et al.*	0.002	0.987	0.033	0.002	0.979	0.040	0.002	0.987	0.035
Newton	0.004	0.964	0.057	0.005	0.956	0.064	0.004	0.963	0.058

Table 5 Results of statistical analysis on Page model

Temp. (°C)	Thickness (mm)	k(min^{-1})	N	χ^2	R^2	RMSE
	2	0.002	1.131	0.0007	0.991	0.0268
40	4	0.001	1.277	0.0002	0.998	0.0150
	6	0.000	1.354	0.0003	0.997	0.0182
	2	1.17×10^{-5}	1.914	0.0005	0.996	0.0214
50	4	8.84×10^{-6}	1.857	0.0011	0.990	0.0322
	6	1.71×10^{-5}	1.763	0.0006	0.995	0.0214
	2	0.000	1.485	0.0006	0.995	0.0232
60	4	0.000	1.488	0.0008	0.992	0.0008
	6	0.001	1.231	0.0002	0.998	0.0123
	2	0.000	1.512	0.0005	0.996	0.0208
70	4	0.000	1.500	0.0010	0.991	0.0306
	6	0.000	1.468	0.0009	0.991	0.0299
	2	0.009	1.106	0.0001	0.999	0.0098
80	4	0.002	1.328	0.0007	0.994	0.0259
	6	0.003	1.215	0.0004	0.996	0.0196
	2	0.003	1.431	0.0001	0.999	0.0091
90	4	0.003	1.369	0.0001	0.999	0.0110
	6	0.001	1.530	0.0004	0.997	0.0180

Note: $MR = \exp(-kt^n)$.

At all drying conditions, the Page model gave the highest R^2 value (0.996) and the lowest x^2 (0.0005) and RMSE (0.0192) values (Table 4) compared to other models used in this study. The experiment moisture ratio and the predicted moisture ratio for Page model are shown in Figure 7 to confirm the accuracy of selection of the Page model at 70 °C. The experimental and predicted moisture ratio values lay around the straight line which fitted perfectly with a straight line dividing the plot area to two equally. This shows that only page model curve has the least variations from the experimental points as compared to others. This clearly demonstrates that this model could be used to explain the thin layer drying behavior of cocoyam. Oladejo (2020) reported that Page model best fitted the drying characteristics of yellow cassava during convective hot air drying of the untreated sample. Page model also best fitted the drying characteristics of pulped fruit of cranberries in freeze-drying reported by Rudy et al. (2015). Tunde-Akintunde (2011) also reported that Page model best described the drying behavior of chilli pepper for sun and solar drying.

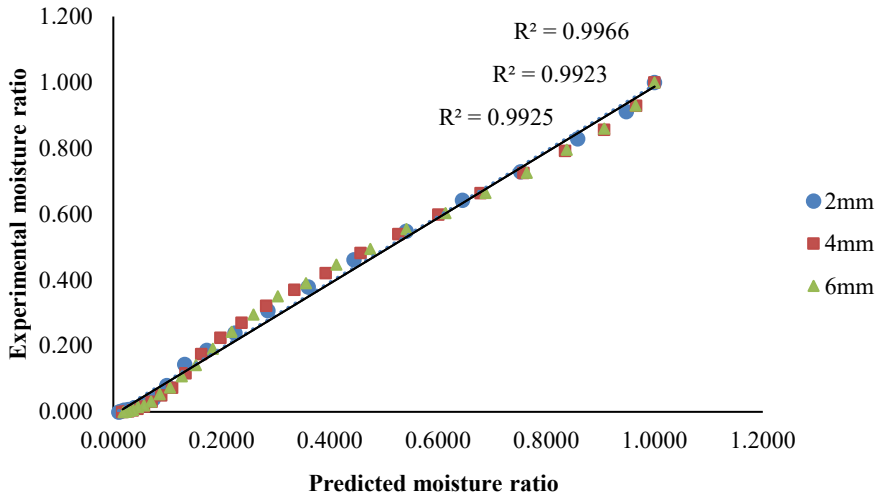

Figure 7 Experimental moisture ratio versus predicted moisture ratio for untreated sample at 70°C

3.6 Effect of drying temperature on cocoyam slices color

The CIELab color parameters for fresh and dried cocoyam corms are presented in Table 6. The L*, a*, b*, Chroma value, total color change (ΔE), browning index (BI) and the Hue angle were reported. The values for the L*, a* and b* coordinates of the fresh cocoyam corms were 84.84, 0.50 and 19.46 respectively. The L* values stand for brightness, the higher the value, the brighter the sample, and the lower the value, the darker. The dried cocoyam slices had lower L^* values (darker color) than the fresh cocoyam slices. This value decreased as the temperature of drying increased from 40°C - 90°C, indicating that high temperature of drying darkens the color of cocoyam slices. There was no significant difference (p>0.05) between the fresh cocoyam slices and cocoyam dried at 40°C. There was no significant difference (p>0.05) between the cocoyam slices dried at 50°C, 60°C, 70°C and 80 °C. However, there was a significant decrease (p<0.05) in the L^* value when the temperature was increased to 90 °C compared to the fresh and samples dried at other temperature, as this temperature had the lowest L^* value. As expected higher temperature darkens the color of cocoyam slices when dried. This is in accordance with the findings of Diamante et al. (2010) for drying of gold kiwifruit, at higher temperature drying causes darkening for gold kiwifruit.

The a^* values fell between 0.56 and 3.58 for fresh to dried cocoyam samples. The a^* values stand for redness, the higher the value, the redder the sample, and the lower values tend to greenness. The fresh samples of cocoyam slices had lower a^* value than the dried samples. The a^* values were observed to increase as the temperature of drying increases. Generally, there was no significant difference (p > 0.05) between the fresh cocoyam slices and sample dried at 40 °C. Similarly, there was no significant difference (p > 0.05) between the samples dried at 50 - 60 °C and between 70 and 80 °C. The high temperature of drying turn the dried products less green (higher a^* values) than the fresh samples. The exposure of the cocoyam slices to high air temperature increases the rate of color degradation as a result of the high energy transferred to the food material. The redder color of the samples may be due to decomposition of chlorophyll and other pigments, and non-enzymatic reactions (Maskan, 2001). Guiné and Barroca (2012) stated that vegetables (pumpkin and green pepper) dried at higher temperature turned the final product less green.

The b^* values range from yellowness to blueness for high to low values, respectively. There was significant (p < 0.05) reduction in the b^* (yellowness) of the dried cocoyam slices compared to the fresh

sample. However, there was no significant difference (p >0.05) between samples dried at 40°C - 90°C. Drying was seen to decrease the yellowness appearance of cocoyam indicating more browning reaction caused by high temperature. Similar increase in the browning index has been reported by Ndisya et al. (2020) for purple-specked cocoyam slices dried from 40°C to 75°C.

Table 6 Effect of temperature on color of cocoyam slices

Temperature (℃)	L^*	a^*	b^*	Chroma	ΔE	Hue	BI
Fresh	84.84 ± 2.87^c	0.56 ± 0.53^a	25.62 ± 1.30^b	25.80 ± 1.22^b	–	88.34 ± 1.66^c	25.88 ± 1.69^a
40	74.46 ± 2.81^c	0.79 ± 0.65^a	19.46 ± 1.40^a	19.47 ± 1.40^a	18.66 ± 1.61^a	84.18 ± 4.10^{abc}	43.75 ± 0.80^b
50	62.37 ± 3.64^b	1.46 ± 0.74^{ab}	17.63 ± 1.93^a	17.90 ± 2.22^a	41.57 ± 4.61^c	81.28 ± 4.86^{ab}	36.21 ± 8.29^{ab}
60	61.61 ± 3.47^b	1.76 ± 0.38^{ab}	17.36 ± 1.61^a	17.47 ± 1.68^a	28.49 ± 4.36^b	84.29 ± 3.22^{abc}	35.04 ± 5.90^{ab}
70	57.71 ± 0.29^b	2.49 ± 0.41^{bc}	17.36 ± 266^a	17.41 ± 2.71^a	32.85 ± 0.25^b	86.49 ± 3.06^{bc}	35.48 ± 8.49^{ab}
80	56.40 ± 1.13^b	2.81 ± 0.48^{bc}	15.28 ± 0.82^a	15.39 ± 0.86^a	44.73 ± 5.35^c	83.46 ± 1.11^{abc}	33.23 ± 1.76^{ab}
90	43.97 ± 7.65^a	3.58 ± 0.49^c	14.13 ± 3.11^a	14.35 ± 3.20^a	45.52 ± 7.88^c	80.21 ± 1.82^a	41.90 ± 3.57^b

Note: Values are represented as means ± standard deviation of triplicate. Means in the same column bearing different superscript differed significantly (p<0.05).

The Chroma value measures the color intensity and saturation of the samples (Pataro et al., 2015). The Chroma values ranged from 14.13 to 25.80 for dried and fresh samples. Samples dried at 40 to 90 °C were significantly lower than the fresh samples. However, there was no significant difference (p >0.05) between the Chroma values of dried cocoyam slices within the temperature of study (40°C to 90°C). The Chroma values decreased with increase in drying temperature from the initial fresh samples up to 90°C. Maskan (2001) also reported the decrease of the initial values of chroma for hot air drying of green kiwifruit dried at 80 °C. The alteration in the Chroma values of the fresh and dried cocoyam slices may due to the carotenoid degradation by high temperature (Gonçalves et al., 2007).

The total color change (ΔE) amongst other parameters is used to determine the color difference between processed and dried food (De Medeiros et al., 2016). The total color ranged from 18.66 to 45.52 for 40°C to 90°C respectively. The total color change (ΔE) was higher at high temperature within the temperature of this study. However, there was no significant difference (P > 0.05) between the total color change of 60°C and 70°C and between 50°C, 80°C and 90°C. The largest difference compared to the fresh sample was observed for those that were dried at 90 °C. These suggest that drying had huge impact on the color of cocoyam yam slices especially at high temperature of drying. The faster degradation of color at high temperature could be due to the high energy transferred to the food material. Diamante et al. (2010) also reported that the total color change of dried gold kiwifruit increased with increase in drying temperature. The color change in the dried samples may be due to non-enzymatic Maillard browning, formation of brown pigment and decomposition of chlorophyll and carotenoid pigments during drying (Maskan, 2001). The lowest color difference was found in the samples dried at 40 °C, indicating that the lowest temperature (40°C) could preserve the typical color of the fresh cocoyam and contribute to reduced browning reaction during the drying process.

The hue angle, h°, is used as one of the qualitative parameters of color of processed foods; the value 0° or 360° indicates redness, while 90°, 180° and 270° represent yellowness, greenness and blueness, respectively (Waramboi et al., 2013). The hue angle of fresh cocoyam was about 88.34° which represent a color in the yellow region. The hue angle ranged from 80.21° to 86.49° for the dried samples. There was significant decrease between the hue angle for the fresh samples and sample dried 90°C. The fresh had the highest hue angle, indicating the degradation of the

yellowness of cocoyam with drying.

The browning index ranged from 25.88 to 43.75 observed for the fresh sample and samples dried at 40°C respectively. The browning index for the fresh cocoyam was significantly lower than the dried samples. However, there was no significant difference between the browning index for the fresh sample and samples dried at 50°C, 60°C, 70°C and 80°C and between 40°C, 50°C, 60°C, 70°C, 80°C and 90 °C. The significant difference between the browning index of the fresh sample and the sample dried at 40 and 90 °C indicate that both long time of drying (40°C) and high drying temperature (90°C) have effect on the browning index of cocoyam.

4 Conclusion

Drying time decreased with increasing drying air temperature and decreasing thickness of cocoyam slices. Drying of cocoyam slices occurred in the falling rate period, which indicated that the dominant diffusion mechanism involved in the drying of cocoyam corms in a convective hot air dryer is moisture diffusion. Increase in the drying temperature increased the effective moisture diffusivity from 1.171×10^{-10} to $7.603 \times 10^{-10} m^2 s^{-1}$ over the temperature range of 40 to 90 °C. The biot number showed that both internal and external mass transfer resistance was responsible for the drying mechanism of convective hot air drying. Results of thin layer drying modeling showed that, the Page model could be used to describe the drying characteristics of the cocoyam slices. Results of the effect of temperature on the color parameters of cocoyam showed that higher temperature darkens the color and reduces the yellowness of cocoyam.

Acknowledgement

This work was supported by the department of Agricultural and Food Engineering, University of Uyo, Uyo, Nigeria.

Conflict of Interest

The Authors declare no conflict of interest.

References

Afolabi, T. J., T. Y. Tunde-Akintunde, and J. A. Adeyanju. 2015. Mathematical modeling of drying kinetics of untreated and pretreated cocoyam slices. *Journal of Food Science and Technology*, 52: 2731-2740.

Agrawal, S. G., and R. N. Methekar. 2017. Mathematical model for heat and mass transfer during convective drying of pumpkin. *Food and Bioproducts Processing*, 101: 68-73.

Akoy, E. O. M. 2014. Experimental characterization and modeling of thin-layer drying of mango slices. *International Food Research Journal*, 21(5): 1911-1917.

Alonge, A. F., and O. A. Adeboye. 2012. Drying rates of some fruits and vegetables with passive solar dryers. *International Journal of Agricultural and Biological Engineering*, 5(4): 83–90.

AOAC (Association of Official Analytical Chemists). 2000. *Official Methods of Analysis, Association of Analytical Chemists*. 15th ed. Washington D. C. USA: AOAC.

Çağlar, A., İ. T. Toğrul, and H. Toğrul. 2009. Moisture and thermal diffusivity of seedless grape under infrared drying. *Food and Bioproducts Processing*, 87(4): 292-300.

Correia, A. F. K., A. C. Loro, S. Zanatta, M. H. F. Spoto, and T. M. F. S. Vieira. 2015. Effect of temperature, time, and material thickness on the dehydration process of tomato. *International Journal of Food Science*, 2015: 970724.

Da Silva, W. P., A. F. Rodrigues, C. M. D. P. S. e Silva, D. S. De Castro, and J. P. Gomes. 2015. Comparison between continuous and intermittent drying of whole bananas using empirical and diffusion models to describe the processes. *Journal of Food Engineering*, 166: 230-236.

Da Silva, W. P., C. M. D. P. S. e Silva,F. J. A. Gama, and J. P. Gomes. 2014. Mathematical models to describe thin-layer drying and to determine drying rate of whole bananas. *Journal of the Saudi Society of Agricultural Sciences*, 13(1): 67-74.

Darvishi, H., J. Khodaei, and M. Azadbakht. 2015. The parameters of mass transfer of convective drying in sliced melon. *Journal of Phillipine Aricultural Scientist*, 98(1): 360-372.

Dash, K. K., S. Gope, A. Sethi, and M. Doloi. 2013. Study on thin layer drying characteristics star fruit slices. *International Journal of Agricultural and Food Science*

Technology, 4(7): 679-686.

De Medeiros, R. A. B., Z. M. P. Barros, C.B.O. de Carvalho, E. G. F. Neta, M. I. S. Maciel, and P. M. Azoubel. 2016. Influence of dual-stage sugar substitution pretreatment on drying kinetics and quality parameters of mango. *LWT - Food Science and Technology*, 67: 167–173.

Demirel, D., and M. Turhan. 2003. Air-drying behavior of Dwarf Cavendish and Gros Michel banana slices. *Journal of Food Engineering*, 59(1): 1-11.

Desa, W. N. M., M. Mohammad, and A. Fudholi. 2019. Review of drying technology of fig. *Trends in Food Science and Technology*, 88: 93-103.

Diamante, L. M., R. Ihns, G. P. Savage, and L. Vanhanen. 2010. Short communication: a new mathematical model for thin-layer drying of fruits. *International Journal of Food Science & Technology*, 45(9): 1956-1962.

Dincer, I., and M. M. Hussain. 2002. Development of a new *Bi-Di* correlation for solids drying. *International Journal of Heat and Mass Transfer*, 45(15): 3065-3069.

Dinrifo, R. R. 2012. Effects of pretreatments on drying kinetics of sweet potato slices. *CIGR Journal*, 14(3): 136-145.

El-Beltagy, A., G. R. Gamea, and A. H. Essa. 2007. Solar drying characteristics of strawberry. *Journal of Food Engineering*, 78(2): 456-464.

Erbay, Z., and F. Icier. 2010. A review of thin layer drying of foods: Theory, modeling, and experimental results. *Critical Reviews in Food Science and Nutrition*, 50(5): 441-464.

Figiel, A., and A. Michalska. 2017. Overall quality of fruits and vegetables products affected by the drying processes with the assistance of vacuum-microwaves. *International Journal of Molecular Sciences*, 18(1): 71.

Ghazanfari, A., S. Emami, L. G. Tabil, and S. Panigrahi. 2006. Thin-layer drying of flax fiber: II. Modeling drying process using semi-theoretical and empirical models. *Drying Technol*ogy, 24(12): 1637-1642.

Gonçalves, E. M., J. Pinheiro, M. Abreu, T. R. Brandão, and C. L. M. Silva. 2007. Modeling the kinetics of peroxidase inactivation, color and texture changes of pumpkin (*Cucurbita maxima* L.) during blanching. *Journal of Food Engineering*, 81(4): 693-701.

Górnicki, K., A. Kaleta, and A. Choińska. 2020. Suitable model for thin-layer drying of root vegetables and onion. *International Agrophysics*, 34: 79-86.

Guiné, R. P. F., and M. J. Barroca. 2012. Effect of drying treatments on texture and color of vegetables (pumpkin and green pepper). *Food and Bioproducts Processing*, 90(1): 58-63.

Hashim, N., O. Daniel, and E. Rahaman. 2014. A preliminary study: kinetic model of drying process of pumpkins (*Cucurbita moschata*) in a convective hot air dryer. *Agriculture and Agricultural Science Procedia*, 2(2): 345-352.

Hssaini, L., R. Ouaabou, H. Hanine, R. Razouk, and A. Idlimam. 2021. Kinetics, energy efficiency and mathematical modeling of thin layer solar drying of figs (*Ficus carica* L.). *Scientific Reports*, 11(1): 21266.

Inyang, U. E., I. O. Oboh, and B. R. Etuk. 2018. Kinetic models for drying techniques-food materials. *Advances in Chemical Engineering and Science*, 8(2): 27-48.

Kabuo, N. O., O. S. Alagbaoso, G. C. Omeire, A. I. Peter-Ikechukwu, L. O. Akajiaku, and A. C. Obasi. 2018. Production and evaluation of biscuits from Cocoyam (*Xanthosoma sagittifolium* Cv Okoriko)- wheat composite flour. *Research Journal of Food and Nutrition*, 2(2): 53-61.

Kamal, M. M., M. R. Ali, M. R. I. Shishir, and S. C. Mondal. 2020. Thin-layer drying kinetics of yam slices, physicochemical, and functional attributes of yam flour. *Journal of Food Process Engineering*, 43(8): e13448.

Kaur, K., and A. K. Singh. 2014. Drying kinetics and quality characteristics of beetroot slices under hot air followed by microwave finish drying. *African Journal of Agricultural Research*, 9(12):1036-1044.

Madamba, P. S. 2003. Thin layer drying models for osmotically pre-dried young coconut. *Drying Technology*, 21(9): 1759-1780.

Maskan, M. 2001. Kinetics of color change of kiwifruits during hot air and microwave drying. *Journal of Food Engineering*, 48(2): 169-175.

Meisami-Asl, E., S. Rafiee, A. Keyhani, and A. Tabatabaeefar. 2010. Determination of suitable thin-layer drying curve model for apple slices (variety-Golab). *Plant Omics*, 3(3): 103-108.

Ndisya, J., D. Mbuge, B. Kulig, A. Gitua, O. Hensel, and B. Sturm. 2020. Hot air drying of purple-pecked Cocoyam (*Colocasia esculenta* (*L.*) *Schott*) slices: Optimization of drying conditions for improved product quality and energy savings. *Thermal Science and Engineering Progress*, 18: 100557.

Ndukwu, M. C., C. Dirioha, F. I. Abam, and V. E. Ihediwa. 2017. Heat and mass transfer parameters in the drying of

cocoyam slice. *Case Studies in Thermal Engineering*, 9: 62-71.

Oladejo, A. O. 2020. Process optimization of ultrasound-assisted osmotic dehydration of yellow cassava using response surface methodology. *Journal of Biosystems Engineering*, 45(3): 167-174.

Oladejo, A. O., M. M. Ekpene, D. I. Onwude, U. E. Assian, and O. M. Nkem. 2021. Effects of ultrasound pretreatments on the drying kinetics of yellow cassava during convective hot air drying. *Journal of Food Processing and Preservation*, 45(3): e15251.

Omolola, A. O., A. I. Jideani, and P. F. Kapila. 2014. Modeling microwave-drying kinetics and moisture diffusivity of Mabonde banana variety. *International Journal of Agricultural and Biological Engineering*, 7(6): 107-113.

Onwude, D. I., N. Hashim, R. B. Janius, N. M. Nawi, and K. Abdan. 2016. Modeling the thin-layer drying of fruits and vegetables: A review. *Comprehensive Reviews in Food Science and Food Safety*, 15(3): 559-618.

Pataro, G., M. Sinik, M. M. Capitoli, G. Donsì, and G. Ferrari. 2015. The influence of post-harvest UVC and pulsed light treatments on quality and antioxidant properties of tomato fruits during storage. *Innovative Food Science and Emerging Technologies*, 30: 103-111.

Rayaguru, K., and W. Routray. 2012. Mathematical modeling of thin-layer drying kinetics of stone apple slices. *International Food Research Journal*, 19(4): 1503-1510.

Rayaguru, K., and W. Routray. 2010. Effect of drying conditions on drying kinetics and quality of aromatic *Pandanus amaryllifolius* leaves. *Journal of Food Science and Technology*, 47(6): 668–673.

Renata, C., K. Adie, D.Yu, M. Beverly, C. Neill, B. Zhang, S. Duncan. 2022. Understanding the Role of Overall Appearance and Color in Consumers' Acceptability of Edamame. *Frontiers in Sustainable Food Systems*, *6*(4), 1–8.

Rudy, S., D. Dziki, A. Krzykowski, U. Gawlik-Dziki, R. Polak, R. Rózyło, and R. Kulig. 2015. Influence of pretreatments and freeze-drying temperature on the process kinetics and selected physico-chemical properties of cranberries (*Vaccinium macrocarpon* Ait.). *LWT-Food Science and Technology*, 63(1): 497-503.

Sacilik, K., R. Keskin, and A. K. Elicin. 2006. Mathematical modeling of solar tunnel drying of thin layer organic tomato. *Journal of Food Engineering*, 73(3): 231-238.

Sadeghi, E., K. Movagharnejad, and A. H. Asl. 2019. Mathematical modeling of infrared radiation thin-layer drying of pumpkin samples under natural and forced convection. *Journal of Food Process and Preservation*, 43(12): e14229.

Saxena, J., and K. K. Dash. 2015. Drying kinetics and moisture diffusivity study of ripe jackfruit. *International Food Research Journal*, 22(1): 414-420.

Simal, S., A. Fermenia, J. A. Cárcel, and C. Roselló. 2005. Mathematical modeling of the drying curves of kiwi fruits: Influence of the ripening stage. *Journal of the Science of Food and Agriculture,* 85(3): 425-432.

Tai, N. V., M. N. Linh, and N. M. Thuy. 2021. Modeling of thin layer drying characteristics of "*Xiem*" banana peel cultivated at U Minh district, Ca Mau province, Vietnam. *Food Research*, 5(5): 244-249.

Taylor, P. (2010). A review of thin layer drying of foods : Theory, modeling and experimental results. *Journal of Food Science and Nutrition,* 3: 27-33.

Tunde-Akintunde, T. Y. 2011. Mathematical modelling of sun and solar drying of chilli pepper. *Renewable Energy*, 36(8): 2139-2145.

Tzempelikos, D. A., A. P. Vouros, A. V. Bardakas, A. E. Filios, and D. P. Margaris. 2014. Case studies on the effect of the air drying conditions on the convective drying of quinces. *Case Studies in Thermal Engineering*, 3: 79-85.

Wang, Z., J. Sun, X. Liao, F. Chen, G. Zhao, J. Wu, and X. Hu. 2007. Mathematical modeling on hot air drying of thin layer apple pomace. *Food Research International*, 40(1): 39-46.

Waramboi, J. G., M. J. Gidley, and P. A. Sopade. 2013. Carotenoid contents of extruded and non-extruded sweet potato flours from Papua New Guinea and Australia. *Food Chemistry*, 141(3): 1740–1746.

Wiktor, A., M. Sledz, M. Nowacka, K. Rybak, and D. Witrowa-Rajchert. 2016. The influence of immersion and contact ultrasound treatment on selected properties of the apple tissue. *Applied Acoustics*, 103(Part B): 136–142.

Zielinska, M., and S. Cenkowski. 2012. Superheated steam drying characteristic and moisture diffusivity of distillers' wet grains and condensed distillers' solubles. *Journal of Food Engineering*, 109(3): 627-634.